Intrathermocline eddies in the Southern Indian Ocean

J. J. Nauw,[1] H. M. van Aken,[2] J. R. E. Lutjeharms,[3] and W. P. M. de Ruijter[1]

Received 16 February 2005; revised 6 October 2005; accepted 10 November 2005; published 4 March 2006.

[1] In 2001, two relatively saline intrathermocline eddies (ITEs) were observed southeast of Madagascar at 200 m depth. They are characterized by a subsurface salinity maximum of over 35.8 at potential temperatures between 18° and 22°C. The oxygen concentrations within the high salinity cores are slightly elevated compared with those of the surrounding water. Their horizontal extent is about 180 km, several times the Rossby deformation radius, while their thickness is about 150 m. The observed circulation around the ITEs is anticyclonic and maximum velocities of 20 to 30 cm/s are observed at 200 m depth. In these cores the potential density anomaly ($25.0 < \gamma < 25.9$ kg/m^3) has a relatively low vertical gradient and therefore a low planetary potential vorticity. The hydrographic properties of these ITEs are distinctly different from those of the surrounding thermocline water, and especially from the much fresher water mass in the East Madagascar Current. Strong evidence has been found that the distant formation area of the water mass in the ITEs is the subtropical Southern Indian Ocean east of 90°E and south of 25°S, where Subtropical Underwater (STUW) is formed with similar characteristics. Similar high-salinity cores as the ITEs are also found in the thermocline around 200 m depth along an almost zonal section between Madagascar and 100°E. Differences between the hydrographic properties of these cores and the ITEs near Madagascar may partly be explained by interannual variations in the temperature and salinity of the surface mixed layer water in the possible formation area.

Citation: Nauw, J. J., H. M. van Aken, J. R. E. Lutjeharms, and W. P. M. de Ruijter (2006), Intrathermocline eddies in the Southern Indian Ocean, *J. Geophys. Res.*, *111*, C03006, doi:10.1029/2005JC002917.

1. Introduction

[2] Intrathermocline eddies (ITEs) [*Dugan et al.*, 1982] or subsurface lenses [*Armi and Zenk*, 1984] and submesoscale coherent vortices (SCVs) [*McWilliams*, 1985] have been found in many regions of the world ocean [*Kostianoy and Belkin*, 1989]. ITEs (or lenses) and SCVs have several characteristics in common, although they have probably been formed differently. The features in these two classes have a lens-like shape and are located in the subsurface, intermediate or near-bottom layers of the ocean. Their flow field is primarily horizontal and nearly all of them display an anticyclonic rotation and have a subsurface velocity maximum. They are characterized by a pycnostad over a depth range of the order of 100 to several hundreds of meters in which the chemical properties usually display small vertical gradients. ITEs usually have a horizontal extent of the same size or larger than the internal Rossby radius of deformation, while SCVs are generally much smaller, related to their different generation processes. ITEs and SCVs are long-lived and retain much of the characteristics of their formation area. They often move far from their origin, primarily through advection. Therefore the hydrographic and chemical properties of ITEs and SCVs are often distinct from those of the surrounding thermocline water.

[3] Observations suggest that ITEs are formed at upper ocean fronts [*Riser et al.*, 1986; *Gordon et al.*, 2002] where isopycnals from the thermocline outcrop in the winter mixed layer. There Mode Water is subducted into the thermocline, which does not always ease into the interior, but sometimes forms isolated lenses. These lenses are characterized by vertically homogeneous hydrographic properties embedded in the upper thermocline, hence the name "intrathermocline eddies." For example, the ITEs in the Japan/East China Sea [*Gordon et al.*, 2002] had a salinity of 34.12 and a temperature of about 10°C characteristic for their subpolar origin. They displayed an anticyclonic rotation, were located in the upper thermocline at a depth of 200 m, and had a horizontal and vertical extent of about 100 km and 150 m, respectively. It has been suggested that they were formed through frontal convergence and subduction of winter mixed layer water along the southern edge of the subpolar front.

[4] The formation of the surface mixed layer occurs through mixing processes, which are mainly controlled by buoyancy fluxes and the wind stress imposed by the overlying atmosphere. Part of the mass flux from the mixed layer into the interior of the main thermocline is induced by

[1]Institute for Marine and Atmospheric Research Utrecht, Department of Physics and Astronomy, Utrecht University, Utrecht, Netherlands.
[2]Royal Netherlands Institute for Sea Research, Den Burg, Netherlands.
[3]Department of Oceanography, University of Cape Town, Cape Town, South Africa.

0148-0227/06/2005JC002917$09.00

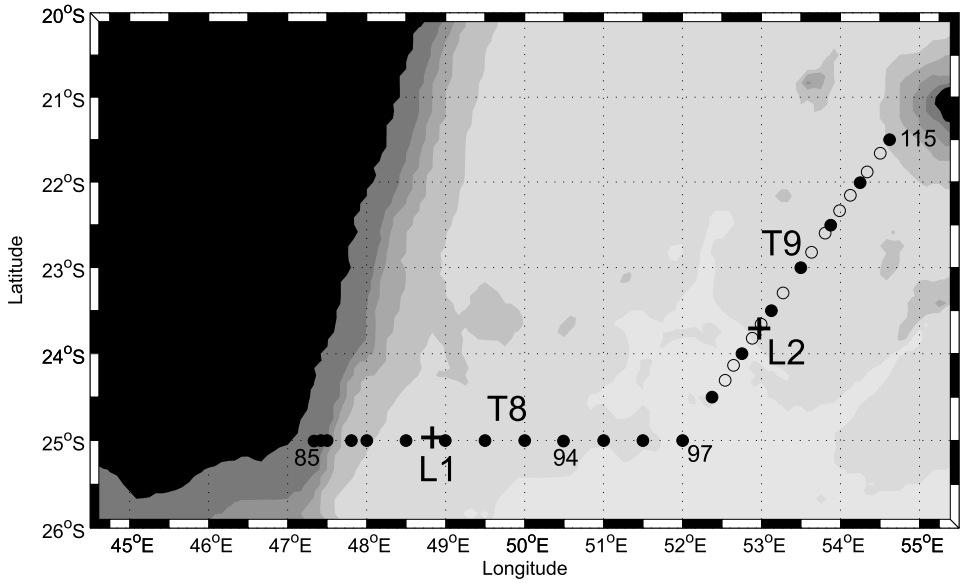

Figure 1. Map of the survey area indicating the locations where hydrographic profiles were taken. Solid circles indicate a CTD station, while open circles indicate XBT stations. The crosses, denoted L1 and L2, indicate the locations where two subsurface ITEs have been observed.

vertical motion set up by a convergent Ekman transport driven by the large-scale wind-stress curl. This occurs primarily in the subtropical convergence zone where the mean wind-stress curl has its maximum. A horizontal cross-frontal flow may also induce a mass flux into the main thermocline if it is directed from a region with a deep winter mixed layer towards a region with a relatively shallow one. Both mechanisms can be of the same magnitude [*Marshall et al.*, 1993].

[5] *Spall* [1995] showed that the process of subduction at upper ocean fronts is primarily caused by growth of baroclinic instabilities, which could trigger regions of frontogenesis. Parcels subducted from a deep surface mixed layer into a much thinner thermocline developed an anticyclonic motion through conservation of potential vorticity. A close resemblance between the subducted parcels and SCVs was pointed out. Moreover, the characteristics of these SCVs were determined by the mechanism of frontogenesis and the depth of the surface mixed layer. A pairing with a cyclonic vortex or the large-scale flow might be able to transport the SCVs for a long distance from their original location of formation [*Riser et al.*, 1986]. *Ou and Gordon* [2002] propose a different scenario for the generation of ITEs in relation to subduction along a mid-ocean front, which is based on steady state balances. Their mechanism poses a potential vorticity constraint on the mixed layer waters. This constraint only allows for part of the mixed layer waters to enter the thermocline, while the rest is dammed up to form anticyclonic eddies. In this case, the size of the eddy is limited by the entrainment rate. Hence, in both of these mechanisms SCVs or ITEs are being formed from surface mixed layer water at a mid-ocean front.

[6] During a survey of the southern termination of the East Madagascar Current (EMC) as part of the Dutch-South African ACSEX programme (Agulhas Current sources experiment) two intrathermocline eddies (ITEs) were detected southeast of Madagascar. The ACSEX research cruise was designed to investigate the circulation near Madagascar and especially the path taken by the southern branch of the EMC. In this paper the characteristics of the ITEs are presented and a possibly distant origin is discussed.

2. Hydrographic Observations of Two Intrathermocline Eddies

[7] During the ACSEX cruise by RV Pelagia several hydrographic sections were surveyed [*van Aken et al.*, 2004] (Figure 1). The southern branch of the East Madagascar Current (EMC) was surveyed with an eastward hydrographic section (T8) perpendicular to the coast of Madagascar. A northeastward section (T9) continued to Reunion Island. The survey of these sections took place between 20 and 24 March 2001. The mean station interval at section T8 was about 27 nautical miles (51 km), and somewhat smaller over the continental slope of Madagascar. On section T9 the distance between successive CTD stations was 36 nautical miles (67 km). Several expendable bathythermograph (XBT) profiles were also taken between the CTD stations of section T9 to improve the horizontal resolution.

[8] On both sections an ITE is present (L1 and L2 in Figure 1) at about 200 m depth, containing a highly saline pycnostad. The distributions of the salinity in the upper 600 dbar along the hydrographic sections (Figures 2a and 3a) reveal the two ITEs as (positive) salinity anomalies at a pressure of 200 dbar. They have a thickness of about 150 m and their horizontal scale along the ship track is about 180 km.

[9] In the centers of the ITEs the salinity exceeds 35.8 about 0.2 higher than that in the surrounding thermocline water (Figures 2a and 2b). Their potential temperature is between 18° and 22°C and displays a low vertical gradient (Figures 2c and 2d). The vertical homogeneity within the

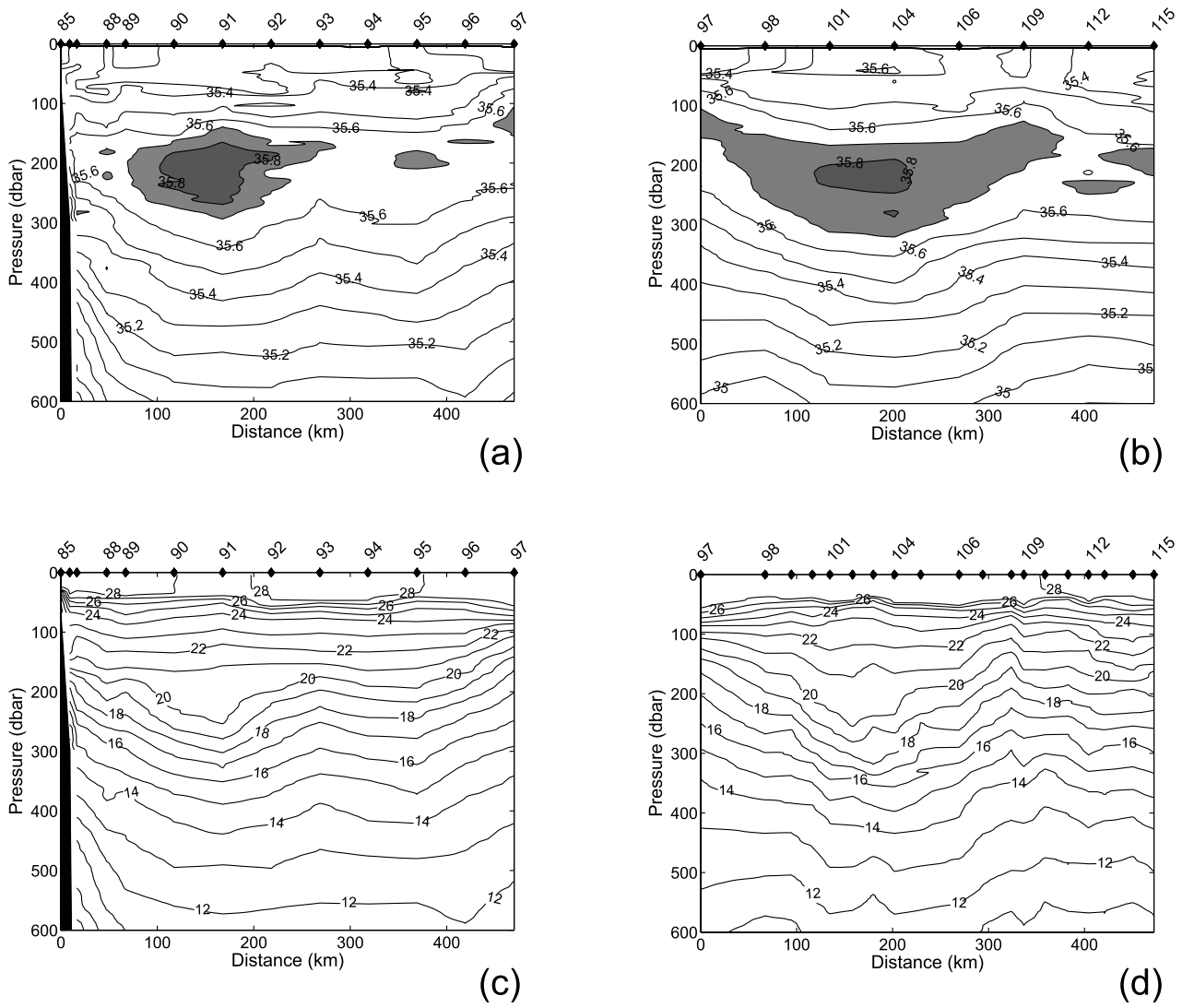

Figure 2. Hydrographic properties along sections T8 and T9 indicated in Figure 1. (a, b) Salinity along sections T8 and T9, respectively. (c) Potential temperature (in °C) along section T8. (d) Temperature (in °C) along section T9.

ITEs is also clearly visible in the distribution of the potential density anomaly, γ, (Figures 3a and 3b), which is between about 25.0 and 25.9 kg/m^3. This is also reflected in the planetary potential vorticity, λ, which is much lower in the ITEs than in the surrounding thermocline (Figures 3c and 3d). The planetary potential vorticity is defined as $\lambda = f\frac{\partial \rho}{\partial z}/\rho = f N^2/g$, where f is the Coriolis parameter, ρ is the density, N is the Brunt–Väisälä frequency and g the gravitational acceleration. This characteristic is clearest in ITE L1, where the potential vorticity minimum exactly coincides with the positive salinity anomaly. The size of the ITEs is several times the internal Rossby radius of deformation, which is slightly over 40 km at this latitude. On section T8, the dissolved oxygen concentration was determined for water samples, taken at 100, 200 and 300 m depth (Figure 4). Within the core of L1 (stations 90 and 91) the oxygen concentration at 200 m is at least 15 μmol/kg higher than in the surrounding thermocline water at the same depth. In the oxygen concentration at 100 and 300 m, just above and below the positive salinity anomaly, this signal is much weaker or even absent. The oxygen concentrations at these levels are generally higher [*Warren*, 1981b]. Unfortunately, the dissolved oxygen data is not available for section T9.

[10] During the survey 1-min ensembles were recorded with a RDI 75-kHz narrow beam Vessel Mounted Acoustic Doppler Current Profiler (VMADCP). From this data 30-min-averaged velocity profiles were determined for each 8-m bin, which leads to an estimated accuracy of 5 cm/s or better. The velocity fields of L1 and L2 display an anticyclonic rotation (Figure 5a). L1 is located at the outer edge of the East Madagascar Current (EMC), which induces anticyclonic shear that may partly obscure the velocity structure of the ITE. Below 400 m the vertical current shear is low (Figure 5a); the velocity at these levels was therefore considered to represent the "background" flow, not disturbed by the ITE. Hence the velocity averaged over a pressure interval between 400 and 538 m was subtracted from the velocity distribution in the upper 400 m assuming to result in a "reduced ITE velocity" (Figure 5c). This reduced velocity distribution

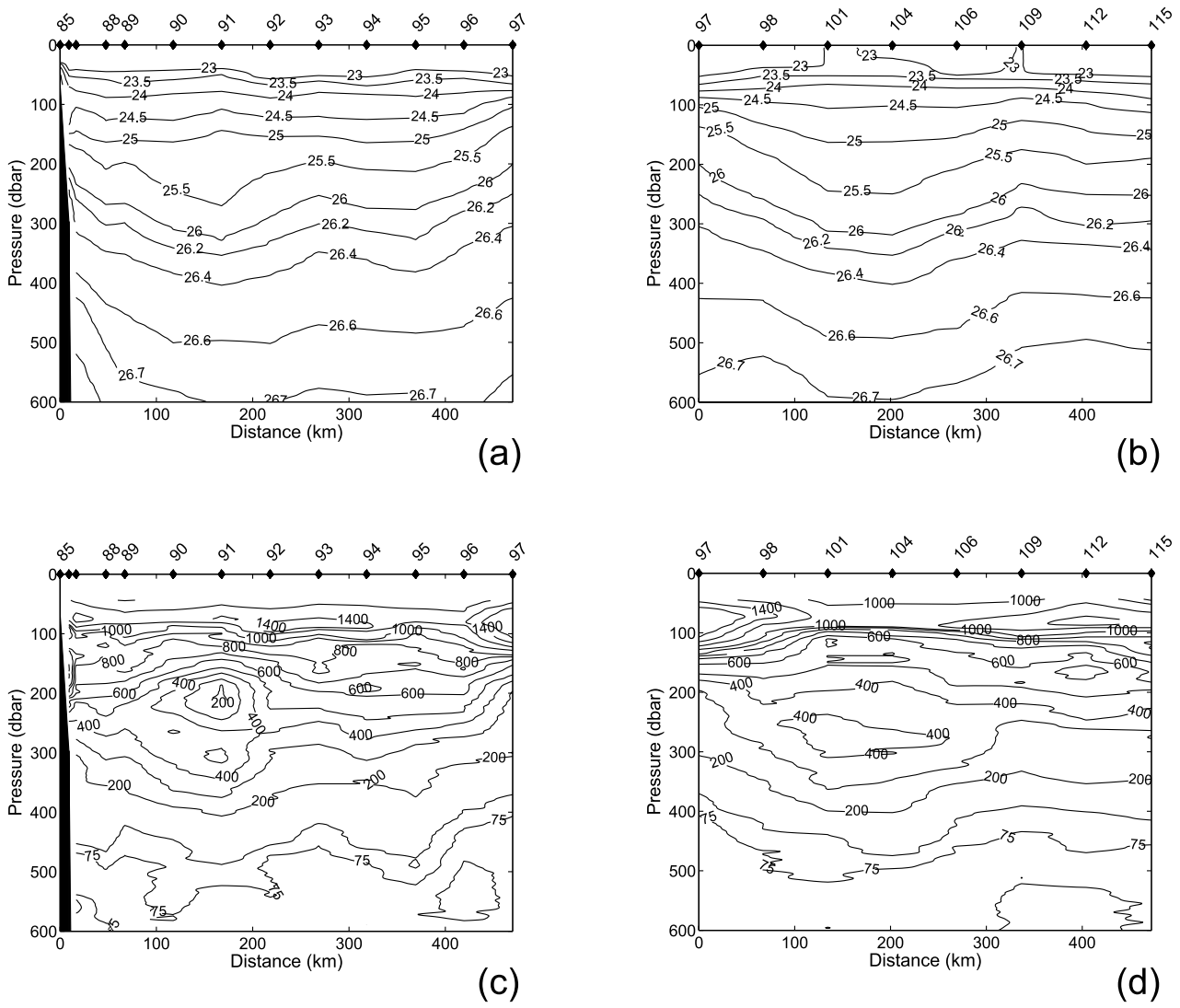

Figure 3. Hydrographic properties along sections T8 and T9 indicated in Figure 1. (a, b) Potential density anomaly, γ, (kg m^{-3}) along sections T8 and T9, respectively. (c, d) Potential vorticity, λ, along these sections in units of 10^{-12} (m s)$^{-1}$.

still shows an anticyclonic circulation at the core depth of the ITEs. The maximum reduced velocity observed at the edge of ITE L1 exceeded 20 cm/s. The velocities induced by the presence of ITE L2 even exceeded 30 cm/s (Figures 5b and 5d). The influence of the ITEs is also visible in the near-surface velocity field. The velocity structures measured with a Lowered ADCP attached to the CTD frame (not shown) reveal an anticyclonic circulation extending to about 1000 m depth which is most likely induced by the presence of the ITEs. This implies that the use of the average velocity between 400 and 538 m as a background velocity might underestimate the reduced ITE velocity.

[11] Nearby tracks of the TOPEX/Poseidon and ERS-2 satellites at the time of the survey showed sea surface height (SSH) anomalies of 8 and 12 cm relative to the large-scale surface topography which could be related to the presence of ITEs L1 and L2, respectively (Figure 6). The anomalous SSH are only slightly smaller than the magnitude of the dynamic heights of 13 and 22 cm derived from the direct velocities measured with the VMADCP at a depth of 34 m assuming that geostrophy is valid. The length scales of the anomalies along the T/P tracks are also in the order of 100 to 200 km similar to the horizontal scale along the ship track. Hence, apart from other more prominent features, such as the surface intensified eddy centered near 50.5°E and 24.5°S (SSH ≈25 cm, Figure 5a), nonnegligible sea surface height anomalies could be connected to the ITEs.

[12] The ITEs reported here are in several aspects comparable to those observed in the Japan/East China Sea [*Gordon et al.*, 2002]. The latter also displayed an anticyclonic rotation, were located at the same depth of 200 m, and had a similar horizontal and vertical extent. They only had a lower salinity and a lower temperature, which is clearly due to their formation through frontal convergence and subduction of the winter mixed layer along the southern edge of the subpolar front. Hence a similar mechanism for the formation of the warm and saline ITEs near Madagascar through subduction of surface mixed layer water at a surface front somewhere upstream in the Indian Ocean may be suggested. The relatively low potential vorticity within the

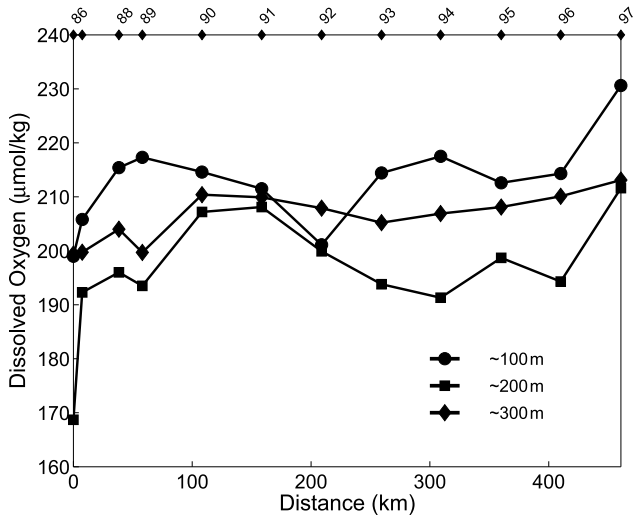

Figure 4. Dissolved oxygen concentration (μmol/kg) at 100, 200, and 300 m depth along section T8 (Figure 1).

ITEs derived from vertically homogeneous mixed layer water is consistent with this hypothesis. The high salinity (and temperature) in the ITEs near Madagascar suggests a near-subtropical source region of the water in the ITEs, which is consistent with the work of *Gordon et al.* [2002], who studied ITEs of subpolar origin.

[13] The position of L1 might suggest a formation of these eddies locally at the eastern front of the EMC. However, the high salinity within the ITE cores (Figure 7) compared with that of the surrounding thermocline water and water of the EMC suggests a more distant origin. In the next section, evidence is sought to support the hypothesis of the formation of these ITEs at a surface front in the Indian Ocean. Therefore areas in the Indian Ocean are sought where mixed-layer water subducts, which have similar hydrographic properties as those of the warm and saline ITEs near Madagascar. Moreover, the possible advection of this subducted mixed-layer water by average surface circulation from the area of subduction towards Madagascar will be investigated.

2.1. Subduction of the Winter Mixed Layer in the Indian Ocean

[14] Because the high-salinity water mass in the core of the ITEs near Madagascar is assumed to be produced by subduction of winter mixed layer water, surface salinities of similar magnitude should be present in some regions of the Indian Ocean. The WOCE hydrographic data (WOCE Data Products Committee, 2000), the data obtained during three hydrographic surveys in 2000 and 2001 within the ACSEX programme [*Ridderinkhof and De Ruijter*, 2003; *De Ruijter et al.*, 2002; *van Aken et al.*, 2004], as well as ARGO float data, were used to identify areas of subduction of saline mixed layer water in the Indian Ocean. To fill up the spatial gaps, pre-WOCE data obtained from the World Ocean Database were added. The maximum salinity and associated depth and temperature were determined for individual profiles that reached to at least 300 m depth. First, we removed obviously erroneous data points, such as maximum salinities lower than 30 (anywhere) or higher than 35.5 in the outflow region of the Indonesian Archipelago. Outliers were filtered out by removing data points that deviated more than 3.3 times the standard deviation from the mean in $5^\circ \times 5^\circ$ squares. This value of 3.3 was chosen to retain the maximum salinity of the profiles through the ITEs near Madagascar.

[15] The maximum salinity (surface or subsurface) for each station clearly shows the relatively fresh Indonesian Throughflow Water (ITFW with $S < 35$) in the South Equatorial Current (SEC) around 10°S (Figure 8a). The location of the saline ITEs south-east of Madagascar, reported in the previous section, can be distinguished by a few orange markers surrounded by less saline waters indicated by mostly yellow and green markers. Two regions with maximum salinities exceeding 35.5 can be observed. One north of the equator close to the Arabian Sea and one in the Southern Hemisphere, stretching all the way from Africa to Australia. In the subtropical region between 35°S and 12°S and east of 75°E the maximum salinity even exceeds 36. The potential density at which the salinity maximum is located in the Southern Indian Ocean, $\gamma \sim 26.0$ kg m^{-3}, is much more comparable to that of the ITEs than its value in the Arabian Sea which is only $\gamma \sim 23.5$ kg m^{-3} (Figure 8c). Moreover, the former area also seems to be a more likely formation area for the water in the ITEs near Madagascar, because there exists a connection between both regions through the westward flowing SEC. The pressure at which the salinity maximum is found (Figure 8b) indicates that this latitude band can be divided into a southern and a northern part. The maximum salinity is found near the surface in the southern part of this latitude band (between 25°S and 35°S), while it is generally observed around 200 dbar between 12°S and 25°S. This region is roughly coincident with the area where Ekman pumping dominates the subduction rates in the Indian Ocean subtropical gyre as can be seen in Figure 2a of *Karstensen and Quadfasel* [2002].

[16] The stations on the meridional WOCE section I9N at 95°E (Figure 9) were sampled between 28 January and 8 February 1995, in the Southern Hemisphere summer [*Gordon*, 1995]. Between 23°S and 25°S, a subsurface frontal zone can be recognized in the distributions of the potential temperature, salinity and density. There the saline subtropical surface water is separated from the fresher surface water of the SEC by the South Indian Tropical Front [*Tchernia*, 1980]. Between 23°S and 18°S, a subsurface saline water mass ($S > 35.9$) is located in the main thermocline between about 100 and 300 m depth. It is directly connected to the surface salinity maximum south of 24°S (Figure 9b). The meridional scale of the subsurface saline water mass is about 1000 km and its vertical scale is of order 150 m. It seems more or less to be confined between the anomalous potential density surfaces of $25.0 < \gamma < 26.2$ kg m^{-3} (Figure 9c). This is similar to the range at which the ITEs were found. The subsurface saline water mass has most likely been formed by subduction of a surface mixed layer formed in the south. A high dissolved oxygen concentration might be expected in this layer, because of its likely recent contact with the atmosphere. However, between 100 and 400 dbar at the location of the high-salinity core a relative oxygen minimum is observed in the vertical (Figure 9d) probably owing to in situ oxygen

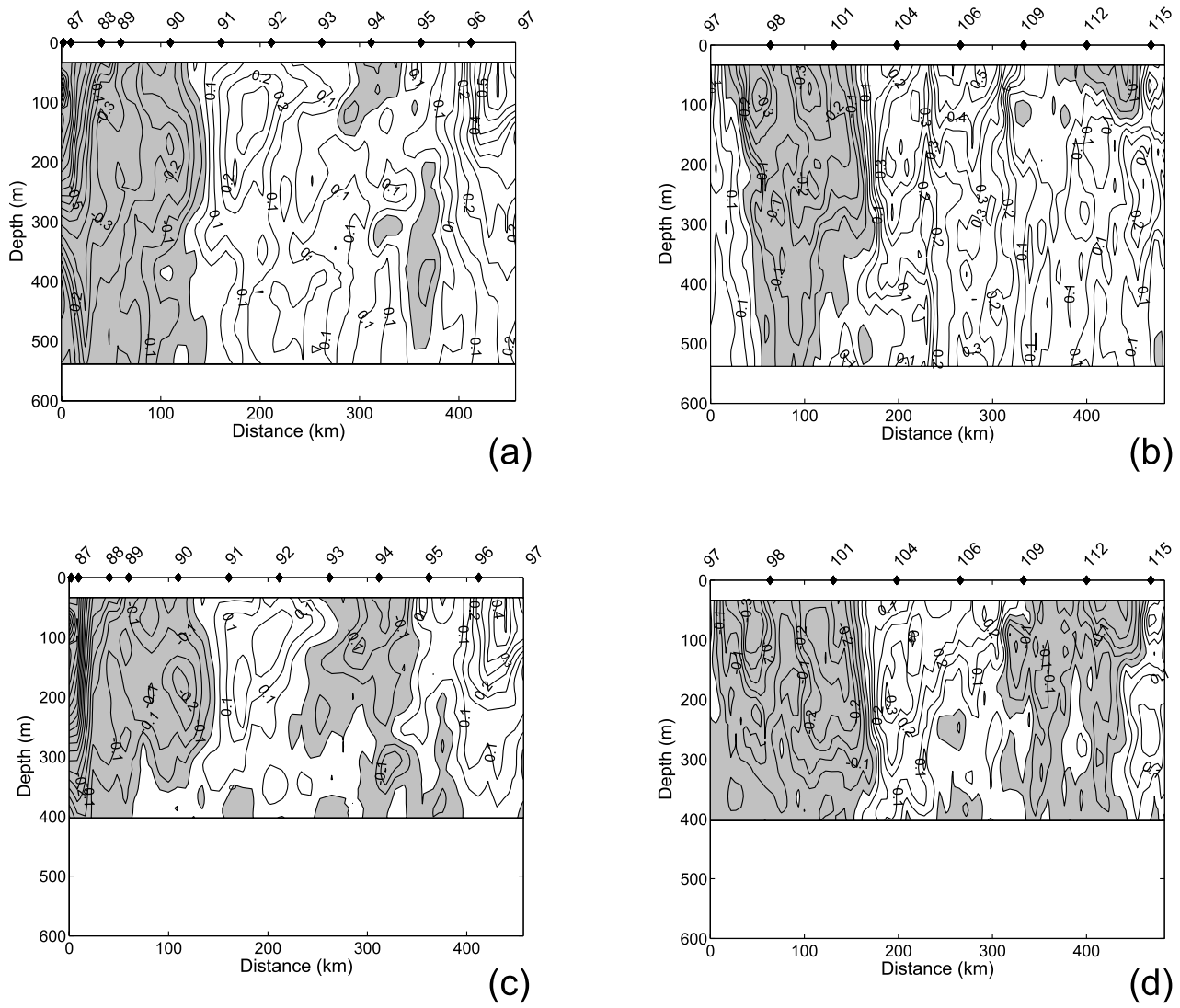

Figure 5. (a, b) Velocity distribution (m/s) perpendicular to section T8 and T9, respectively, measured with the Vessel Mounted ADCP (VMADCP). (c, d) Velocity anomaly relative to the depth-averaged perpendicular flow between 400 and 538 dbar for sections T8 and T9, respectively.

consumption [*Warren*, 1981b]. At about 200 dbar a front in the oxygen distribution is present between 16°S and 18°S, coinciding with a strong horizontal gradient in the salinity (Figures 9b and 9d). The low dissolved oxygen concentration (<160 μmol/kg) together with the relatively low salinity (S <35.4) of the water north of this front indicate the presence of ITFW [*Gordon*, 1986; *Godfrey*, 1996]. The small-scale structures in the salinity and oxygen distributions between 12°S and 19°S around 200 m depth are correlated with each other and represent isopycnal intrusions of ITFW and STUW in the frontal zone.

2.2. Westward Advection of Subtropical Underwater

[17] The subducted saline subtropical water identified in the previous section is called Subtropical Underwater (STUW) [*Hanawa and Talley*, 2001]. In all subtropical oceans, high-salinity surface water is formed in high evaporation regions after which it subducts at a tropical front where it meets low-saline tropical or equatorial water (in the North Atlantic [e.g., *Worthington*, 1976]; in the South Pacific [e.g., *Tsuchiya and Talley*, 1998]; and in the Indian Ocean [e.g., *Wyrtki*, 1973; *Warren*, 1981a; *Toole and Warren*, 1993; *Talley and Baringer*, 1997]). Because of its formation history, a subsurface salinity maximum associated with the STUW might be expected in every ocean. Although it is common in all subtropical oceans, its formation and relative importance to the circulation of the upper thermocline has not received a lot of attention, except in a recent study by *O'Connor et al.* [2002], who determined its formation rate both in the North and South Pacific.

[18] The subduction of STUW at the tropical front may be accompanied by the formation of ITEs of STUW by either the proposed mechanism of *Spall* [1995] or of *Ou and Gordon* [2002]. Local instabilities of the SEC, which carries the STUW westward, might also be a cause for the formation of isolated saline ITEs. The circulation in the southern part of the Indian Ocean is characterized by a basin-wide anticyclonic subtropical gyre [*Stramma and*

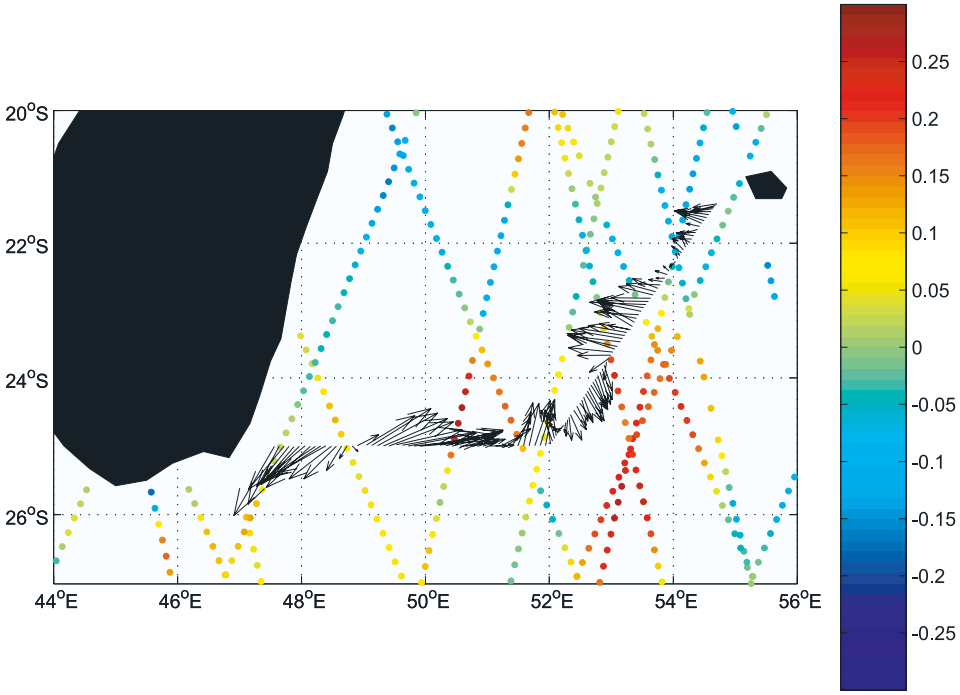

Figure 6. Alongtrack sea surface height (SSH) anomalies measured by the TOPEX/Poseidon and ERS-2 satellites between 18 and 26 March 2001. Superposed are vectors of direct velocity measurements with the VMADCP at 202 m depth.

Lutjeharms, 1997]. At about 10°S, fresher Indonesian Throughflow water is introduced into the gyre and forms the northward boundary of the subtropical waters in the SEC. The westward flowing SEC advects the STUW, including possible locally formed ITEs, toward Madagascar. Hydrographic data near 20°S along the nearly zonal WOCE section I3 between Madagascar and Australia [*Howe and Bindoff*, 2000] was used to analyze whether ITEs, containing this eastern type of STUW, were present in the SEC farther east near Madagascar. The stations on this section were occupied in the austral autumn of 1995. Between 86°E and 99°E, three isolated high-salinity patches were centered at a depth of about 200 m (Figure 10b). The maximum salinity in the patches increased slightly to the east and exceeded 35.9 in the center of the most eastern high-salinity core near 97°E. The horizontal distance between the high-salinity patches was about 450 km and their temperature was between 17° and 20°C (Figure 10a). The entire band with high salinity STUW is located between the anomalous potential density of $25.0 < \gamma < 26.2$ kg m^{-3} (Figure 10c). The dissolved oxygen concentration in the layer with STUW was relatively low compared with the layers above and below (Figure 10d), which may have been caused by in situ oxygen consumption after subduction [*Warren*, 1981b]. At this point it cannot be decided whether the high-salinity water masses are actual isolated ITEs or part of a meandering SEC.

[19] Farther west along section I3, up to the EMC near Madagascar, similar high-salinity patches appear to be located in the top of the main thermocline. Between 57°E and 86°E the salinity as well as the horizontal scale of these patches decreased. The salinity in the core of the high-salinity patches on the same I3 section close to Madagascar between 49°E and 57°E decreased to well below 35.7 (Figure 11b). However, this salinity still remains about 0.2 larger than the salinity of the waters in the surrounding thermocline water. Moreover, the temperature in these patches was slightly warmer than in the ones farther east,

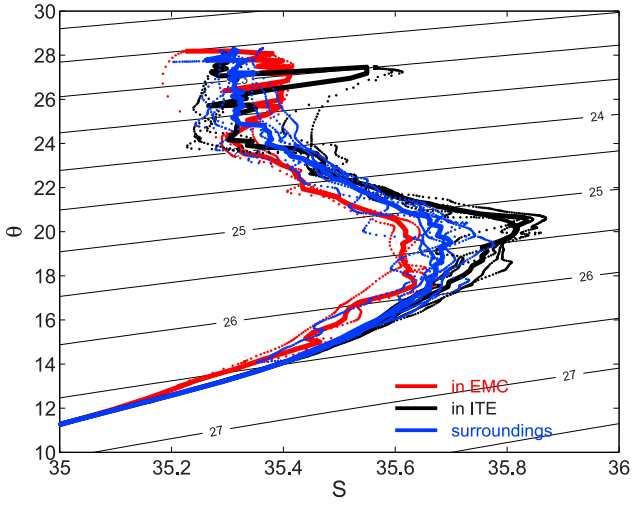

Figure 7. The θ-S diagram for hydrographic properties along sections T8 and T9. The red dotted lines display θ-S properties within the EMC (at stations 85, 86, and 87), black dotted lines display θ-S properties in the core of the ITEs (stations 90, 91, 92, 101, and 104), and blue dotted lines display θ-S properties in the waters directly surrounding the ITEs (stations 88, 94, 95, 96, 112, and 115). Stations near the edge of the ITEs are assumed to have mixed hydrographic properties and are therefore not shown. The drawn lines show the regional mean θ-S diagram, where properties have been averaged along isopycnals.

i.e. between 18° and 21°C (Figure 11a). However, they are also between the anomalous potential density surfaces of $25.0 < \gamma < 26.2$ (Figure 11c).

[20] Note that both the salinity within the patches on section I3 as well as in the surrounding waters were about 0.2 lower than the salinity observed on sections T8 and T9 during the ACSEX cruise in 2001 (Figure 2), while the latter measurements were taken only 5° farther to the south. Hence either the salinity in the western part of the Indian Ocean increased between 1995 and 2001 or a large meridional salinity gradient is present. The difference between the maximum and minimum salinity at a depth of 200 dbar between 20°S and 25°S along the meridional section I7C at 54.5°E, sampled in July of 1995 [*Donohue and Toole*, 2003], was only about 0.08. Moreover, this difference was mainly caused by the presence of similar high-salinity patches as those observed along section I3. Furthermore, along 32°S a salinification of the upper thermocline waters was also observed between 1987 and 2002 [*Talley and Baringer*, 1997; *Bryden et al.*, 2003]. This suggests that a trend in salinity may have occurred in upper thermocline waters in the entire western part of the Southern Indian Ocean.

[21] The dissolved oxygen concentration in the saline water masses is much higher than in their surroundings (Figure 11d). The low dissolved oxygen concentration (<170 μmol/kg) and low salinity in the surrounding waters indicates the presence of diluted ITFW. Diluted ITFW was apparently transported southward to intrude between the high-salinity patches. This seems to enhance the difference between the characteristics in the high-salinity patches and the waters in their immediate surroundings. This difference is best reflected by investigating the depth-averaged properties in the maximum salinity layer, i.e., averaged over the anomalous potential density range of $25.0 < \gamma < 26.2$ kg m^{-3}. This revealed a salinity difference of 0.1 between the patches and their surroundings in the eastern part of WOCE section I3 (Figure 10b) and almost 0.2 in the western part of this section (Figure 11b). Associated with this, also an enhanced temperature difference between the patches and their immediate surroundings near Madagascar as compared with the ones east of 86°E seemed to be caused by these intrusions.

[22] There appears to be a correspondence between the θ-S properties in the cores of the high-salinity patches observed on section I3 close to Australia and the average properties of the warm and saline ITEs near Madagascar (Figure 12). The maximum salinity of the former only occurs at a somewhat lower temperature than the maximum salinity observed in the warm and saline ITEs near Madagascar. This maximum may have shifted to higher temperature and lower density when colder less saline water from the thermocline below mixes with water of the saline patch during the advective transport by the

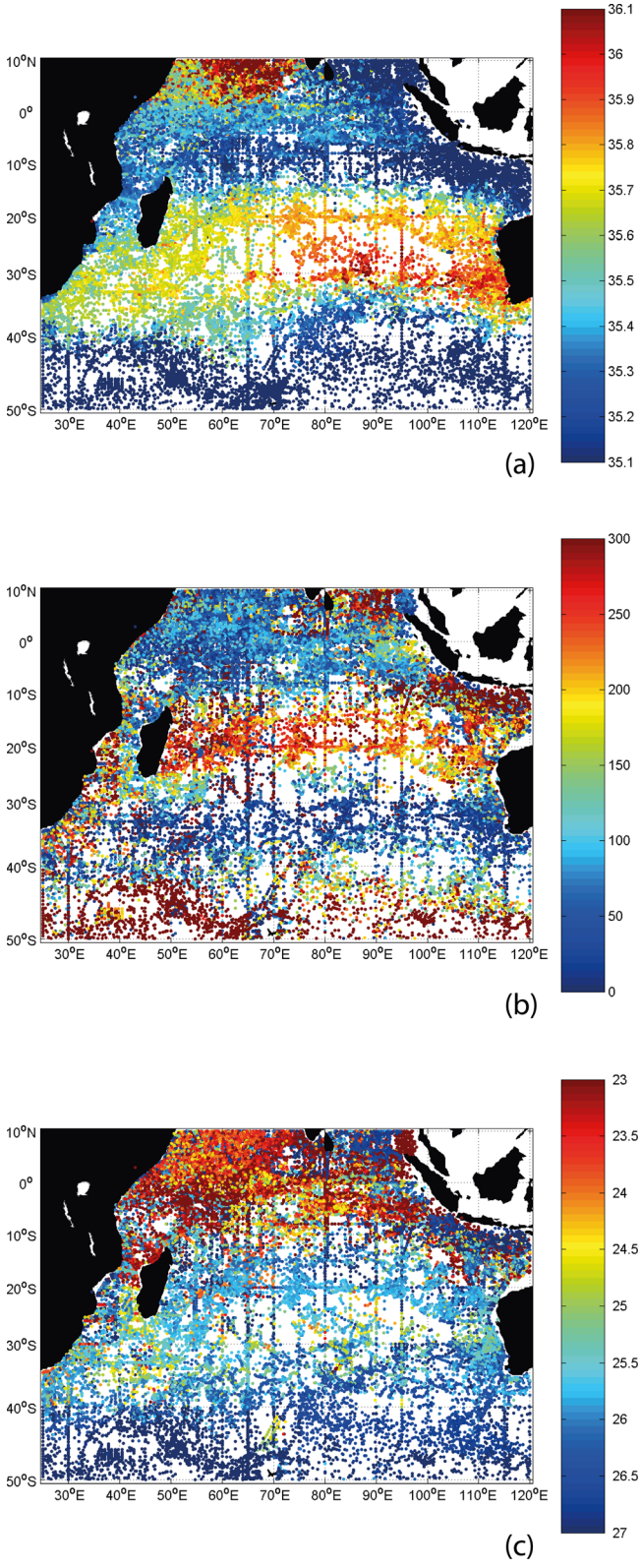

Figure 8. (a) Surface and subsurface salinity maxima for the hydrographic data observed during the WOCE, ACSEX, and ARGO programs, supplemented with pre-WOCE data from the World Ocean Database (2001). Blue indicates a salinity maximum of 35 or less, and red indicates 36 or more. (b) Local pressure at which the salinity maxima occur. Red indicates a pressure of 300 dbar or more, while blue indicates that the salinity maximum was already observed at the surface. (c) Potential density at which the salinity maxima occur. Red indicates an anomalous potential density of $\gamma <= 23.0$ kg m^{-}3, and blue indicates $\gamma >= 27.0$ kg m^{-3}.

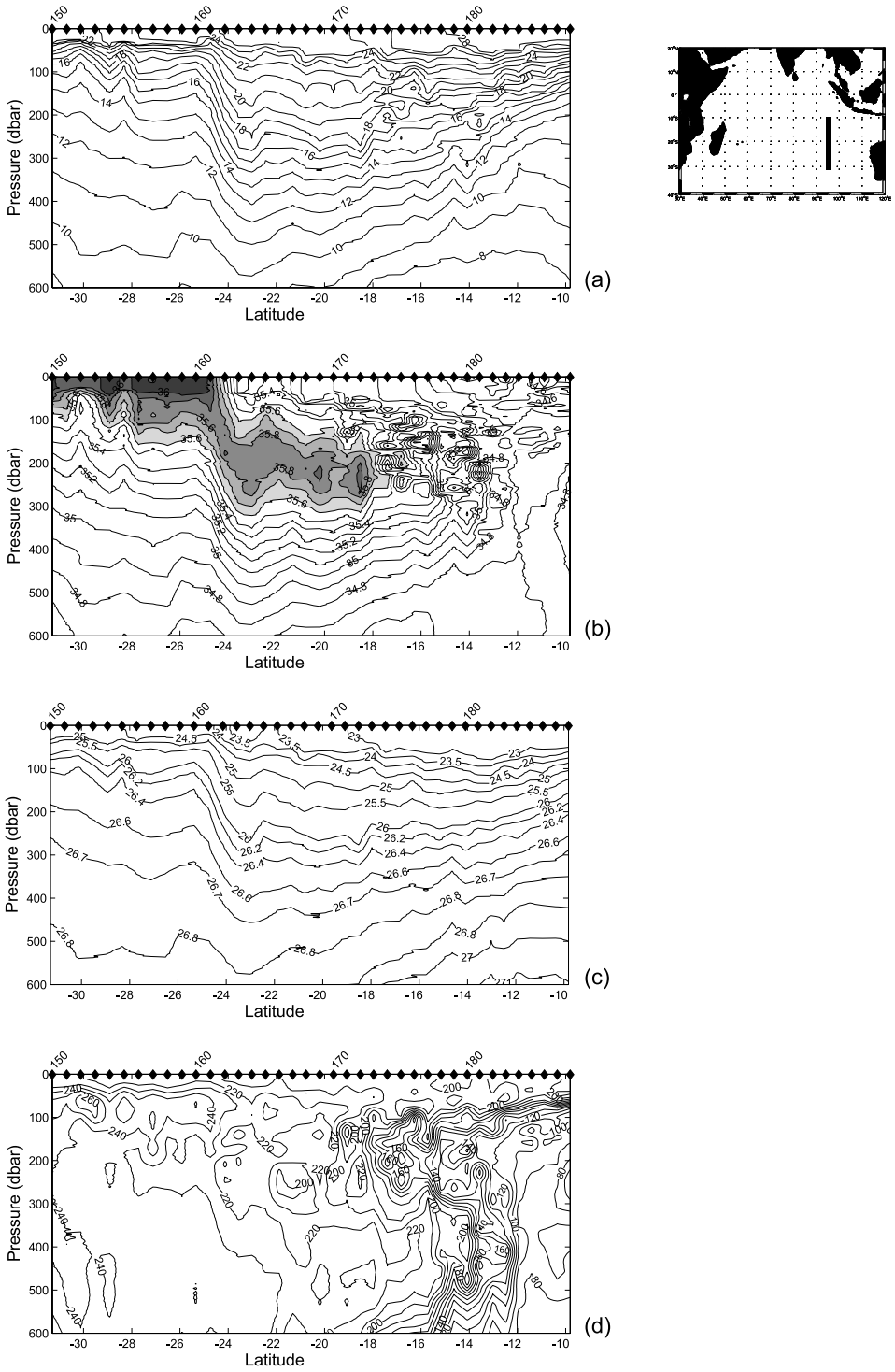

Figure 9. Hydrographic properties along the part of WOCE section I9N: (a) temperature (°C); (b) salinity; (c) anomalous potential density; and (d) dissolved oxygen concentration smoothed in the vertical with a 13-point running average (i.e., over 26 dbar in μmol/kg).

SEC. Comparison of the θ-S properties of the ITEs near Madagascar (solid lines in Figure 12) with those observed on section I9N (Figure 9) suggests that water mass in the ITEs originate from at least east of 90°E.

[23] A possible explanation for the differences between the high-salinity patches on section I3 and the ITEs may be interannual variations in the θ-S properties of the subtropical surface winter mixed layer. An ITE that is formed from (part of) this (subducted) winter mixed layer water will have inherited its hydrographic properties. Therefore the annual minima in the sea surface temperature (SST) and associated sea surface salinity (SSS) south of the South Indian Tropical

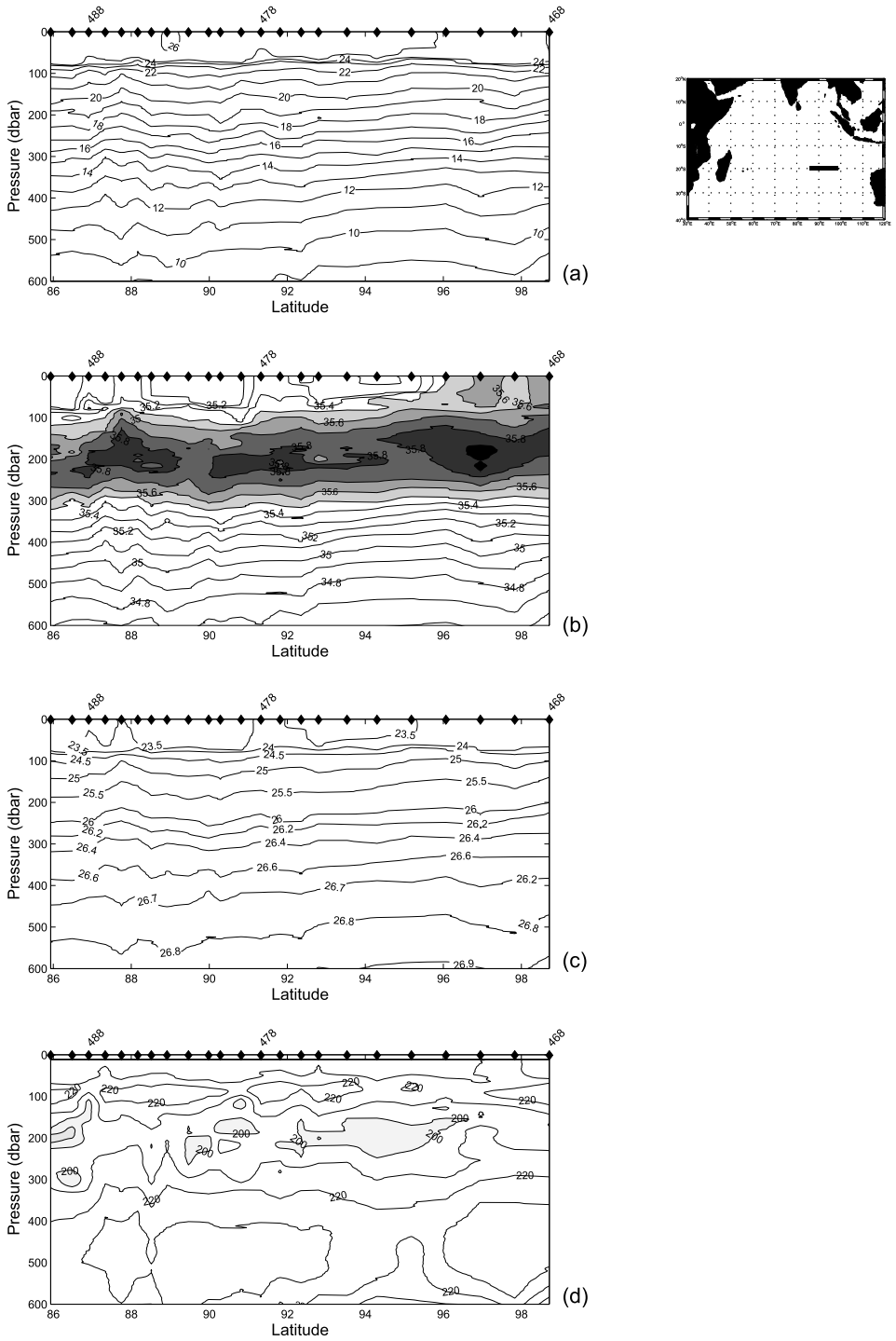

Figure 10. Hydrographic properties along the a part of WOCE section I3 between 86° and 99°E: (a) temperature; (b) salinity; (c) anomalous potential density; and (d) dissolved oxygen concentration smoothed in the vertical with a 13-point running average (i.e., over 26 dbar in μmol/kg).

Front might be similar to the hydrographic properties of the subducted waters and/or ITEs. The time series of the monthly SST and SSS obtained from the *Reynolds et al.* [2002] (in red) and *Levitus et al.* [2005] and *Boyer et al.* [2005] (in black) data sets averaged over the area between 25°S and 30°S and 80°E and 100°E clearly show considerable interannual variations (Figure 13). The northern boundary of this area represents the approximate mean location of the front (not shown); the other boundaries are chosen based on the results of Figure 8. The seasonal values for the SST and SSS based on the WOD data interpolated at 90°E and 27.5°S are plotted as blue dots for comparison. The mean minimum SST is 18.70° ± 0.28° and 18.74° ± 0.35° for the *Reynolds et al.* [2002] and *Levitus et al.* [2005] data set, respectively. The correspondence between these values provides confidence that both data sets represent the

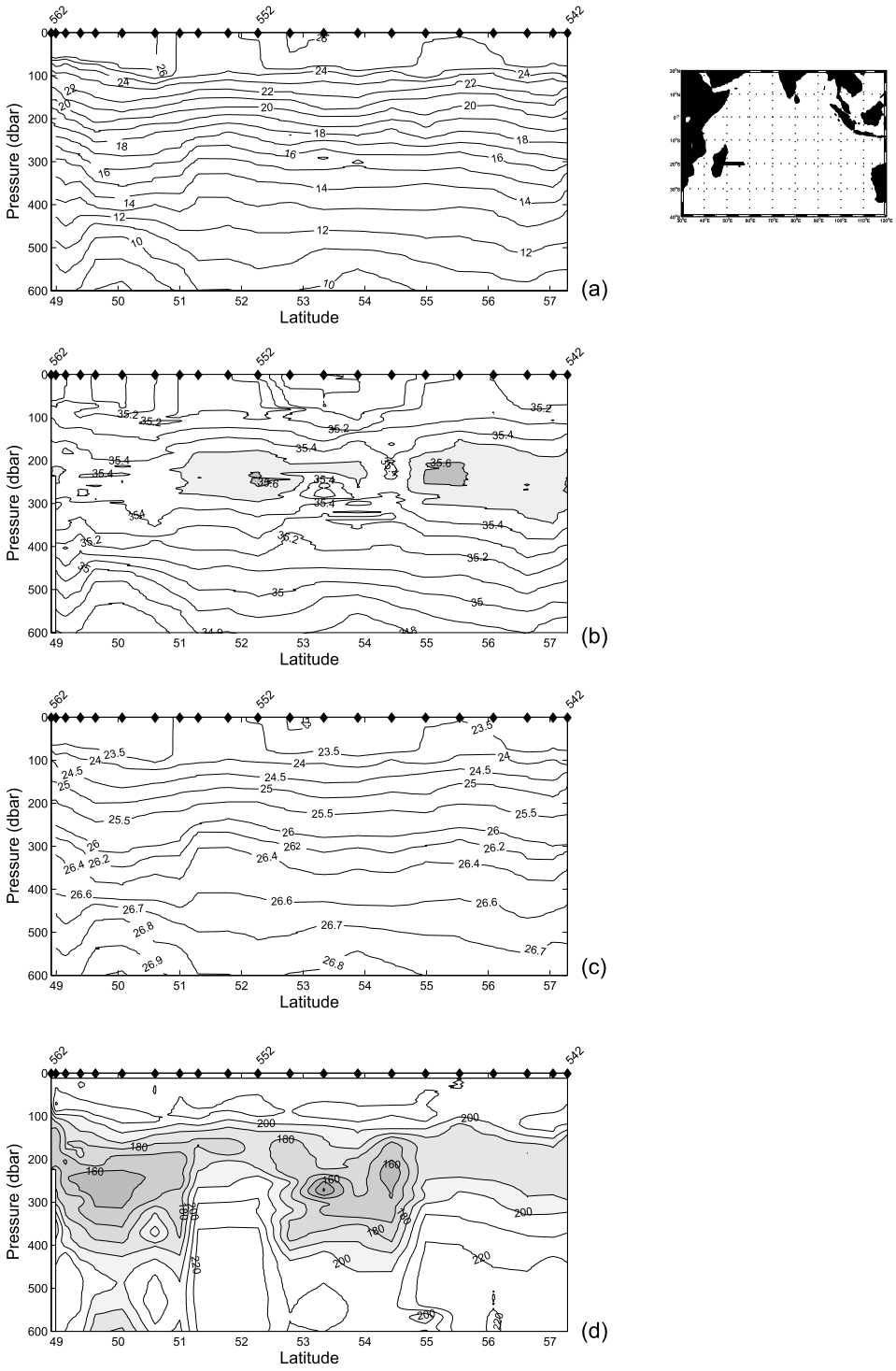

Figure 11. Hydrographic properties along the a part of WOCE section I3 between 49° and 57°E: (a) temperature; (b) salinity; (c) anomalous potential density; and (d) dissolved oxygen concentration smoothed in the vertical with a 13-point running average (i.e., over 26 dbar in μmol/kg).

true SST. These mean minimum SST values are also very similar to the temperature at the maximum salinity in the patches on section I3 (Figure 12). The temperature of the ITEs (~20.4°C) is obviously outside of the range of SST in the subduction area in the eastern part of the subtropical gyre. However, SST deviations from the mean of as much as a degree Celsius are not exceptional. Moreover, other processes, like diapycnal mixing, may alter the hydrographic properties of the ITEs during their lifetime. The mean SSS associated with the annual minima in the SST is 35.75 ± 0.04, which has a large correspondence with the maximum salinity in the ITEs, although it is less comparable with the high-salinity patches on section I3. Apparently, differences in hydrographic properties of ITEs formed in successive

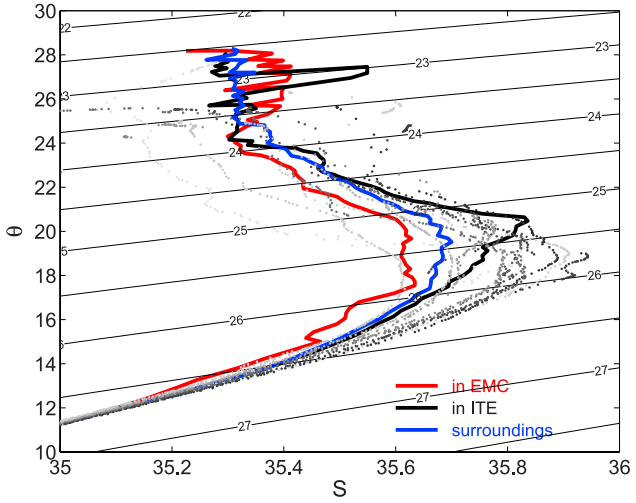

Figure 12. The θ-S diagram for hydrographic properties for stations along section I3 that display a local salinity maximum in the horizontal plane. The grayscale corresponds to the longitude at which these stations are taken; dark gray corresponds to stations close to Australia, while light gray corresponds to stations near Madagascar. The drawn lines show the average θ-S diagrams for the hydrographic properties near Madagascar during the ACSEX programme, reproduced from Figure 7.

years may partly be explained by interannual variations in the hydrographic properties of the surface mixed layer waters in the eastern part of the South Indian subtropical gyre.

3. Summary and Discussion

[24] Two intrathermocline eddies (ITEs) were observed southeast of Madagascar just seaward of the southern branch of the East Madagascar Current (EMC). These ITEs had a diameter of approximately 180 km, which is several times the local Rossby radius of deformation, and a thickness of about 150 m. They were located in the thermocline at a depth of about 200 m. The salinity within the center of these ITEs exceeded 35.8, which was at least 0.2 higher than the salinity in the surrounding thermocline water. The potential temperature in the ITEs varied between 18° and 22°C. The vertical density gradient in these ITEs was relatively small, which was reflected by their relatively low (planetary) potential vorticity compared with their surroundings. Velocity measurements showed an anticyclonic motion associated with these ITEs. The maximum azimuthal velocity was between 20 and 30 cm/s and occurred at the edges of the ITEs at their core depth. The anticyclonic motion was not restricted to this depth, but (although strongly reduced) could be observed near the surface and at a depth of about 1000 m. This might be a coincidence, but it seems that the ITEs have an effect on the dynamics over much larger depths than their vertical extent.

[25] The formation of these ITEs locally within the EMC seems very unlikely, since the waters of the EMC are much fresher than those within the ITEs, which had led to the hypothesis of a distant origin. The structure of the ITEs reported here have similar characteristics as the ITEs found in the Japan/East China Sea [*Gordon et al.*, 2002]. The latter also displayed an anticyclonic rotation, were located at the same depth of 200 m, and had a similar horizontal and vertical extent. However, the ITEs in the Japan/East China Sea are characterized by a lower salinity and a lower temperature compared with their immediate surroundings. These cold and fresh ITEs in the Japan/East China Sea were suggested to be formed by frontal convergence and subduction of winter surface mixed layer water at the southern edge of the subpolar front. Similarly, our analysis of the WOCE, WOD, ARGO and ACSEX data in the Indian Ocean indicates that the warm and saline ITEs near Madagascar seem to originate from saline subtropical mixed layer water.

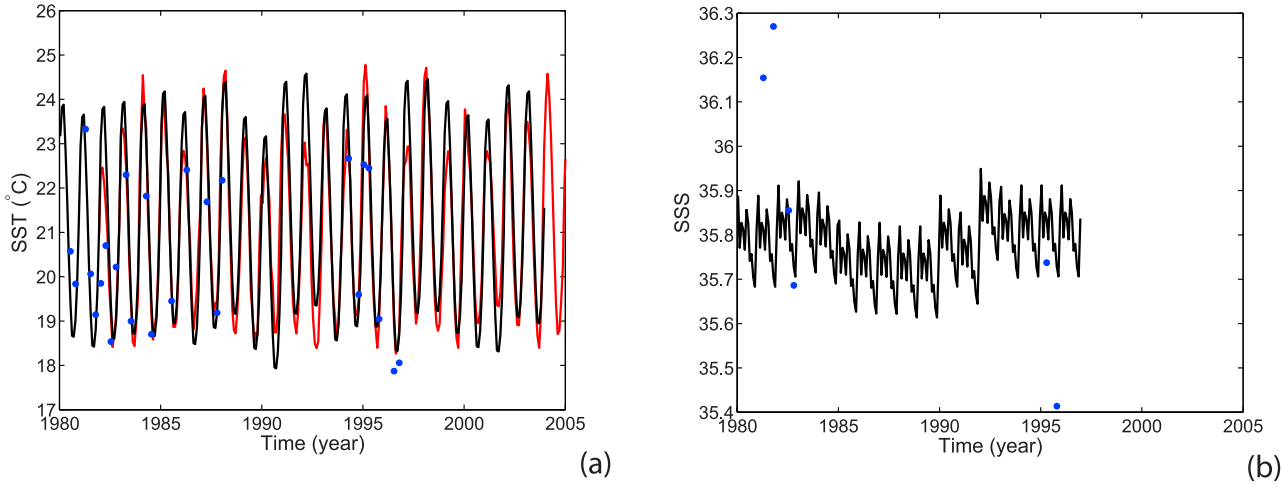

Figure 13. Time series of (a) sea surface temperature (SST) and (b) sea surface salinity (SSS) averaged over the area between 80°E and 100°E and 25°S and 30°S. The red line shows the monthly SST from the *Reynolds et al.* [2002] data set, while the black lines are composed from the *Levitus et al.* [2005] and *Boyer et al.* [2005] data sets, for SST and SSS, respectively. The blue dots show the seasonally averaged values at 90°E and 27.5°E interpolated from the data obtained from the World Ocean Database (2001).

[26] The process of subduction of saline subtropical surface mixed layer water along the South Indian Tropical Front between the tropics and subtropics has been shown to occur in the eastern part of the subtropical gyre in the Southern Indian Ocean. The water mass properties of this Subtropical Underwater (STUW) closely match those of the ITEs near Madagascar. There are only small differences in salinity and density between the STUW and the ITEs. Large (interannual) variations in wintertime sea surface temperature and salinity in the eastern part of the subtropical gyre may partly explain these differences. Besides this, also turbulent mixing with surrounding water while the ITEs are moving westward might change the hydrographic properties within the ITEs.

[27] The east-west section I3 at 20°S observed during WOCE displayed a series of patches with a positive salinity anomaly which had a size of several 100 km, of the same order as the diameter of the ITEs. Low salinity and low oxygen (diluted) Indonesian Throughflow Water (ITFW) seemed to have been drawn between the patches close to Madagascar, increasing the differences between the hydrographic properties of the patches and their surrounding thermocline water. The properties of the subsurface saline patches east of Madagascar on I3 seem to be controlled by the water originating from the Subtropical Eastern Indian Ocean gyre not by the fresher water with an equatorial origin: ITFW. Hence this hydrographic section revealed a link between the subduction area in the eastern part of the subtropical gyre and the location near Madagascar where the ITEs were observed.

[28] Two mechanisms have been proposed for the formation of ITEs by *Spall* [1995] and *Ou and Gordon* [2002]. Both are associated with the subduction of mixed layer water across an upper ocean front. Moreover, also instabilities of the SEC may possibly generate ITEs. With the mechanism of *Spall* [1995] relatively small ITEs (or more precisely SCVs) are formed with the size of the Rossby radius of deformation. The ITEs created by the mechanism of *Ou and Gordon* [2002] can become larger, because their size depends on the available excess of mixed layer water. Hence we believe that the latter is the most likely formation mechanism, because high-salinity cores are already visible close to the subduction area near 100°E. This is clearly speculation, since the available data are insufficient to answer the question of what causes the formation of the ITEs presented in this paper.

[29] Subduction of saline subtropical surface water at a tropical front and the formation of STUW is common in all subtropical oceans [*Hanawa and Talley*, 2001]. Moreover, isolated cores of STUW have also been observed in the Pacific [*Tsuchiya and Talley*, 1998]. This suggests that the presence of ITEs may be a common phenomenon in the subtropics and is possibly important in the transport of subtropical water over long distances.

[30] The path that will be taken by the ITEs, after their passage of south Madagascar, is unclear. They will probably be advected by the EMC southward and westward around Madagascar. They may even be involved in the formation of the anticyclonic member of the dipole eddy pairs observed South of Madagascar [*De Ruijter et al.*, 2004], because their velocity structure is not bounded to the near surface, but seems to reach all the way to about 1000 m. If so, we can speculate that they move into the Agulhas region [*Schouten et al.*, 2002] and may explain the high near-surface salinity observed in the western part of the 32°S WOCE section [*Toole and Warren*, 1993]. There they might contribute to the high salinity of the Agulhas Current itself and eventually become a source of salt for an Agulhas ring entering into the Atlantic [*De Ruijter et al.*, 1999; *van Aken et al.*, 2003].

[31] **Acknowledgments.** This investigation was funded by: Netherlands Organisation for Scientific Research via its CLIVAR(NET) programme; Royal Netherlands Institute of Sea Research; Institute of Marine and Atmospheric Research Utrecht, Utrecht University, and the University of Cape Town. The pre-WOCE data were obtained from the World Ocean Database (2001, http://www.nodc.noaa.gov/OC5), and the WOCE data came from the WOCE International Project Office, Southampton, U.K. (2000, DVD-ROM, version 3.0). The ARGO float data were collected and made freely available by the International Argo Project and the national programmes that contribute to it http://www.argo.ucsd.edu, http://argo.jcommops.org). We thank Peter Jan van Leeuwen, Mathijs Schouten, and the anonymous reviewers for their suggestions on this work. Furthermore, the crew of the RV Pelagia and all who sailed on the ACSEX II cruise are gratefully acknowledged.

References

Armi, L., and W. Zenk (1984), Large lenses of highly saline Mediterranean water, *J. Phys. Oceanogr.*, *14*, 1560–1567.

Boyer, T. P., S. Levitus, J. I. Antonov, R. A. Locarnini, and H. E. Garcia (2005), Linear trends in salinity for the world ocean 1955–1998, *Geophys. Res. Lett.*, *32*, L01604, doi:10.1029/2004GL021791.

Bryden, H. L., E. L. McDonagh, and B. A. King (2003), Changes in ocean water mass properties: Oscillations or trends,, *Science*, *300*, 2086–2088.

De Ruijter, W. P. M., A. Biastoch, S. S. Drijfhout, J. R. E. Lutjeharms, R. P. Matano, T. Pichevin, and P. J. Van Leeuwen (1999), Indian-Atlantic interocean exchange: Dynamics, estimation and impact, *J. Geophys. Res.*, *104*(C9), 20,885–20,910.

De Ruijter, W. P. M., H. Ridderinkhof, J. R. E. Lutjeharms, M. W. Schouten, and C. Veth (2002), Observations of the flow in the Mozambique Channel, *Geophys. Res. Lett.*, *29*(10), 1502, doi:10.1029/2001GL013714.

De Ruijter, W. P. M., H. M. van Aken, E. J. Beier, J. R. E. Lutjeharms, P. M. Matano, and M. W. Schouten (2004), Eddies and dipoles around South Madagascar: Formation, pathways and large-scale impact, *Deep Sea Res., Part I*, *51*, 383–400.

Donohue, K. A., and J. M. Toole (2003), A near-synoptic survey of the southwest Indian Ocean, *Deep Sea Res., Part II*, *50*, 1893–1931.

Dugan, J. P., R. R. Mied, P. C. Mignerey, and A. F. Schuetz (1982), Compact, intrathermocline eddies in the Saragasso Sea, *J. Geophys. Res.*, *87*(C1), 385–393.

Godfrey, J. S. (1996), The effect of the Indonesian throughflow on ocean circulation and heat exchange with the atmosphere: A review, *J. Geophys. Res.*, *101*(5), 12,217–12,238.

Gordon, A. L. (1986), Interocean exchange of thermocline water, *J. Geophys. Res.*, *91*(C4), 5037–5047.

Gordon, A. L. (1995), WHP Indian Ocean I9N, *Int. WOCE Newsl.*, *20*, 26–27.

Gordon, A. L., C. F. Guilivi, C. M. Lee, A. Bower, H. H. Furey, and L. Talley (2002), Japan/East Sea intrathermocline eddies, *J. Phys. Oceanogr.*, *32*, 1960–1974.

Hanawa, K., and L. D. Talley (2001), Mode waters, in *Ocean Circulation and Climate: Observing and Modelling the Global Ocean*, edited by G. Siedler, J. Church, and J. Gould, pp. 373–392, Elsevier, New York.

Howe, S. F., and N. L. Bindoff (2000), Decadal differences in the Indian Ocean WOCE I3 section: Water mass changes from the 1960s to 1995, *Int. WOCE Newsl.*, *40*, 6–8.

Karstensen, J., and D. Quadfasel (2002), Water subducted into the Indian Ocean subtropical gyre, *Deep Sea Res., Part II*, *49*, 1441–1457.

Kostianoy, A. G., and I. M. Belkin (1989), A survey of observations on intrathermocline eddies in the world ocean, in *Mesoscale/Synoptic Coherent Structures in Geophysical Turbulence*, edited by J. Nihoul and B. Jamart, pp. 821–841, Elsevier, New York.

Levitus, S., J. I. Antonov, and T. P. Boyer (2005), Warming of the world ocean, 1955–1998, *Geophys. Res. Lett.*, *32*, L02604, doi:10.1029/2004GL021592.

Marshall, J. C., A. J. G. Nurser, and R. G. Williams (1993), Inferring the subduction rate and period over the North Atlantic, *J. Phys. Oceanogr.*, *23*, 1315–1329.

McWilliams, J. C. (1985), Submesoscale coherent vortices in the ocean, *Rev. Geophys.*, *23*, 165–182.

O'Connor, B. M., R. A. Fine, K. A. Maillet, and D. B. Olson (2002), Formation rates of subtropical underwater in the Pacific Ocean, *Deep Sea Res., Part I*, *49*, 1571–1590.

Ou, H.-W., and A. L. Gordon (2002), Subduction along a midocean front and the generation of intrathermocline eddies: A theoretical study, *J. Phys. Oceanogr.*, *32*, 1975–1986.

Reynolds, R. W., N. A. Rayner, T. M. Smith, D. C. Stokes, and W. Wang (2002), An improved in situ and satellite SST analysis for climate, *J. Clim.*, *15*, 1609–1625.

Ridderinkhof, H., and W. P. M. De Ruijter (2003), Moored current observations in the Mozambique Channel, *Deep Sea Res., Part II*, *50*, 1933–1955.

Riser, S. C., W. B. Owens, H. T. Rossby, and C. C. Ebbesmeyer (1986), The structure, dynamics, and origin of a small-scale lens of water in the western North Atlantic thermocline, *J. Phys. Oceanogr.*, *16*, 572–590.

Schouten, M. W., W. P. M. De Ruijter, and P. J. Van Leeuwen (2002), Upstream control of Agulhas ring shedding, *J. Geophys. Res.*, *107*(C8), 3109, doi:10.1029/2001JC000804.

Spall, M. A. (1995), Frontogenesis, subduction, and cross-front exchange at upper ocean fronts, *J. Geophys. Res.*, *100*(C2), 2543–2557.

Stramma, L., and J. R. E. Lutjeharms (1997), The flow field of the subtropical gyre of the South Indian Ocean, *J. Geophys. Res.*, *102*(C3), 5513–5530.

Talley, L. D., and M. O. Baringer (1997), Preliminary results from WOCE hydrographic sections at 80°E and 32°S in the central Indian Ocean, *Geophys. Res. Lett.*, *24*, 2789–2792.

Tchernia, P. (1980), *Descriptive Regional Oceanography*, 253 pp., Elsevier, New York.

Toole, J. M., and B. A. Warren (1993), A hydrographic section across the subtropical South Indian Ocean, *Deep Sea Res., Part I*, *40*, 1973–2019.

Tsuchiya, M., and L. D. Talley (1998), A Pacific hydrographic section at 88°W: Water-property distribution, *J. Geophys. Res.*, *103*(C6), 12,899–12,918.

van Aken, H. M., A. K. Van Veldhoven, C. Veth, W. P. M. De Ruijter, P. J. Van Leeuwen, S. S. Drijfhout, C. P. Wittle, and M. Rouault (2003), Observations of a young Agulhas ring, Astrid, during MARE in March 2000, *Deep Sea Res., Part II*, *50*, 167–195.

van Aken, H. M., H. Ridderinkhof, and W. P. M. De Ruijter (2004), North Atlantic Deep Water in the south-western Indian Ocean, *Deep Sea Res., Part I*, *51*, 755–776.

Warren, B. A. (1981a), Transindian hydrographic section at Lat. 18°S: Property distributions and circulation in the South Indian Ocean, *Deep Sea Res., Part A*, *28*, 759–788.

Warren, B. A. (1981b), The shallow oxygen minimum of the South Indian Ocean, *Deep Sea Res., Part A*, *28*, 859–864.

Worthington, L. (1976), On the North Atlantic circulation, *Johns Hopkins Oceanogr. Stud.*, *6*, 110 pp.

Wyrtki, K. (1973), Physical oceanography of the Indian Ocean, in *The Biology of the Indian Ocean*, edited by B. Zeitzschel, pp. 18–36, Springer, New York.

W. P. M. de Ruijter and J. J. Nauw, Institute for Marine and Atmospheric research Utrecht, Utrecht University, Princetonplein 5, NE-3584 CC Utrecht, Netherlands. (w.p.m.deruijter@phys.uu.nl; j.j.nauw@phys.uu.nl)

J. R. E. Lutjeharms, Department of Oceanography, University of Cape Town, 7700 Rondebosch, Cape Town, South Africa. (johann@ocean.uct.ac.za)

H. M. van Aken, Royal Netherlands Institute for Sea Research, P.O. Box 59, NE-1790 AB Den Burg/Texel, Netherlands. (aken@nioz.nl)